Unambiguous determination of the neutrino mass hierarchy using reactor neutrinos

Yu-Feng Li, Jun Cao, Yifang Wang, and Liang Zhan

Institute of High Energy Physics, Chinese Academy of Sciences, Beijing 100049, China

Determination of the neutrino mass hierarchy in a reactor neutrino experiment at the medium baseline is discussed. Observation of the interference effects between the Δm^2_{31} and Δm^2_{32} oscillations enables a relative measurement independent of the knowledge of the absolute mass-squared difference. With a 20 kton liquid scintillator detector of the $3\%/\sqrt{E \text{ (MeV)}}$ energy resolution, the Daya Bay II experiment at a baseline of ~ 50 km from reactors of total thermal power 36 GW can determine the mass hierarchy at a confidence level of $\Delta \chi^2_{\text{MH}} \sim (10 \div 12) \ (3 \div 3.5\sigma)$ in six years after taking into account the real spatial distribution of reactor cores. We show that the unknown residual energy nonlinearity of the liquid scintillator detector has limited impact on the sensitivity due to the self-calibration of small oscillation peaks. Furthermore, an extra increase of $\Delta \chi^2_{\text{MH}} \simeq 4(9)$ can be obtained, by including the precise measurement of the effective mass-squared difference $\Delta m^2_{\mu\mu}$ of expected relative error 1.5% (1%) from ongoing long-baseline muon neutrino disappearance experiments. The sensitivities from the interference and from absolute measurements can be cross-checked. When combining these two, the mass hierarchy can be determined at a confidence level of $\Delta \chi^2_{\text{MH}} \sim (15 \div 20) \ (4\sigma)$ in six years.

I. INTRODUCTION

An unexpectedly large value of neutrino mixing angle θ_{13} was measured by the Daya Bay reactor neutrino experiment (DYB) [1,2], together with other consistent evidence from the reactor [3,4] and accelerator [5,6] neutrino experiments. It opens a gateway to the measurement of the neutrino mass hierarchy (i.e., the sign of Δm^2_{31} or Δm^2_{32}) and the leptonic *CP*-violating phase (δ_{CP}). A large value of θ_{13} makes both of the above measurements easier in the next generation of neutrino oscillation experiments. Possible information on the neutrino mass hierarchy (MH) can be extracted not only from the matter-induced oscillations of long-baseline accelerator neutrino experiments [7–9] and atmospheric neutrino experiments [10,11], but also from the vacuum oscillation in reactor neutrino experiments at medium baseline [12–23].

The MH sensitivity of a future reactor neutrino experiment comes from the interference effect of two separated oscillation modes [15,16] (i.e., two fast oscillations driven by Δm^2_{31} and Δm^2_{32}). The relative sizes of $|\Delta m^2_{31}|$ and $|\Delta m^2_{32}|$ and the nonmaximal value of θ_{12} make it possible to determine the MH in vacuum, immune from the uncertainty of the Earth density profile and ambiguity of the *CP*-violating phase in atmospheric and long-baseline accelerator neutrino oscillation experiments. Such a measurement is challenging. The energy resolution as the size of $\Delta m^2_{21}/|\Delta m^2_{31}|$ and event number of several tens of thousands are the minimal requirements [16]. Moreover, the spatial distribution of reactor cores [19–21] and nonlinearity of the energy response [23] may also degrade the MH sensitivity.

Besides the interference effect in neutrino vacuum oscillations, direct measurements of the flavor-dependent

effective mass-squared differences (i.e., Δm^2_{ee}, $\Delta m^2_{\mu\mu}$, and $\Delta m^2_{\tau\tau}$) [24,25] may also include the MH information. Δm^2_{ee} from short baseline reactor neutrino experiments (i.e., Daya Bay [26]) and $\Delta m^2_{\mu\mu}$ from the long-baseline accelerator muon-neutrino disappearance are different combinations of Δm^2_{31} and Δm^2_{32}. A reactor neutrino experiment at the medium baseline can measure both Δm^2_{31} (or Δm^2_{32}) and Δm^2_{21} up to the MH sign. Therefore, a comparison of the effective mass-squared differences in different oscillation scenarios can discriminate the neutrino MH. Considering the MH determination from the Daya Bay II reactor neutrino experiment, the sensitivity from the interference effect can be improved by including the accurate measurement of the effective mass-squared difference $\Delta m^2_{\mu\mu}$ from accelerator neutrino experiments or Δm^2_{ee} from reactor neutrino experiments.

Such a study has not been done before and makes sense at least in the following four aspects: (a) we do the first analysis of the nonlinearity effect with explicit nonlinearity functions; (b) we propose the new idea of nonlinearity self-calibration to reduce the nonlinearity effect; (c) our strategy to improve the MH sensitivity using the effective neutrino mass-squared differences is different from previous publications; (d) we discuss the effect of baseline differences and provide the real baseline distribution of the approved Daya Bay II experiment.

The outline of this work is planned as follows. We first give a brief description of the effective mass-squared differences in different oscillation channels in Sec. II. Statistical analysis of Daya Bay II is introduced in Sec. III. Impact from the energy nonlinearity of the liquid scintillator detector is discussed in Sec. IV. Improved MH sensitivity with the absolute mass-squared difference Δm^2_{ee}

and external $\Delta m_{\mu\mu}^2$ measurements is presented in Sec. V. Finally, we conclude in Sec. VI.

II. EFFECTIVE MASS-SQUARED DIFFERENCES

In the standard three-neutrino mixing scheme, the survival probability for the α-flavor neutrinos is given by [27]

$$
\begin{aligned}
P(\nu_\alpha \to \nu_\alpha) \\
= P(\bar{\nu}_\alpha \to \bar{\nu}_\alpha) = 1 - 4|U_{\alpha3}|^2|U_{\alpha1}|^2\sin^2\Delta_{31} \\
- 4|U_{\alpha3}|^2|U_{\alpha2}|^2\sin^2\Delta_{32} - 4|U_{\alpha2}|^2|U_{\alpha1}|^2\sin^2\Delta_{21},
\end{aligned}
\tag{1}
$$

where $\Delta_{ij} = \Delta m_{ij}^2 L/4E$, $\Delta m_{ij}^2 = m_i^2 - m_j^2$, and $U_{\alpha i}$ is the element of the leptonic mixing matrix. Note that only two of the three Δ_{ij} are independent because we have the relation $\Delta m_{31}^2 = \Delta m_{32}^2 + \Delta m_{21}^2$ from their definitions.

Strong hierarchy (i.e., $\Delta m_{21}^2 \ll |\Delta m_{31}^2|$) between the magnitudes of Δm_{21}^2 and Δm_{31}^2 (or Δm_{32}^2) is achieved from the analysis of solar (or KamLAND) and atmospheric (or long-baseline accelerator) neutrino oscillation data [28–30]. To separate the fast and slow oscillation modes, we can rewrite the probability in Eq. (1) as

$$
\begin{aligned}
P(\nu_\alpha \to \nu_\alpha) \\
= 1 - 4|U_{\alpha3}|^2(1 - |U_{\alpha3}|^2)\sin^2\Delta_{\alpha\alpha} \\
- 4|U_{\alpha3}|^2|U_{\alpha1}|^2 \sin[(1 - \eta_\alpha)\Delta_{21}] \sin[2\Delta_{\alpha\alpha} \\
+ (1 - \eta_\alpha)\Delta_{21}] + 4|U_{\alpha3}|^2|U_{\alpha2}|^2 \sin[\eta_\alpha\Delta_{21}] \\
\times \sin[2\Delta_{\alpha\alpha} - \eta_\alpha\Delta_{21}] - 4|U_{\alpha2}|^2|U_{\alpha1}|^2\sin^2\Delta_{21},
\end{aligned}
\tag{2}
$$

where an effective mass-squared difference is defined as the linear combination of Δm_{31}^2 and Δm_{32}^2,

$$
\begin{aligned}
\Delta m_{\alpha\alpha}^2 &\equiv \eta_\alpha\Delta m_{31}^2 + (1 - \eta_\alpha)\Delta m_{32}^2 = \Delta m_{32}^2 + \eta_\alpha\Delta m_{21}^2 \\
&= \Delta m_{31}^2 - (1 - \eta_\alpha)\Delta m_{21}^2,
\end{aligned}
\tag{3}
$$

and $\Delta_{\alpha\alpha} = \Delta m_{\alpha\alpha}^2 L/4E$. We can choose proper values of η_α to eliminate the terms in the second and third lines of Eq. (2), and therefore keep the independent fast and slow oscillation terms. In general, η_α is not only the function of neutrino mass and mixing parameters, but also the function of the neutrino energy and the baseline.

At the first oscillation maximum of the atmospheric mass-squared difference, we have $\Delta_{21} \ll 1$ and the corresponding oscillation effect is extremely small. Expanding to the linear term of Δ_{21}, we can obtain an effective two-neutrino oscillation scheme if the parameter η_α satisfies the following relation:

$$
\eta_\alpha \simeq \frac{|U_{\alpha1}|^2}{|U_{\alpha1}|^2 + |U_{\alpha2}|^2}.
\tag{4}
$$

In a neutrino oscillation experiment of this type, such as the short baseline reactor neutrino experiment (i.e., Daya Bay)

or the long-baseline accelerator muon-neutrino disappearance experiment, it is impossible to distinguish between the two neutrino mass hierarchies because two degenerate solutions with identical $|\Delta m_{\alpha\alpha}^2|$ but different hierarchies can generate the identical neutrino energy spectrum. The absolute values of Δm_{31}^2 (or Δm_{32}^2) in the two solutions are different due to nonzero Δm_{21}^2. The value of η_α varies for different oscillation channels due to the flavor-dependent amplitudes in the oscillation probabilities, so the degeneracy of the neutrino MH can be removed by comparing the effective mass-square differences of different neutrino flavors [24,25].

Using the standard parametrization of the leptonic mixing matrix [27], we get the effective mass-squared differences in Eq. (3) for different channels of neutrino oscillations

$$
\Delta m_{ee}^2 \simeq \cos^2\theta_{12}\Delta m_{31}^2 + \sin^2\theta_{12}\Delta m_{32}^2,
\tag{5}
$$

$$
\begin{aligned}
\Delta m_{\mu\mu}^2 \simeq \sin^2\theta_{12}\Delta m_{31}^2 + \cos^2\theta_{12}\Delta m_{32}^2 \\
+ \sin2\theta_{12}\sin\theta_{13}\tan\theta_{23}\cos\delta\Delta m_{21}^2,
\end{aligned}
\tag{6}
$$

$$
\begin{aligned}
\Delta m_{\tau\tau}^2 \simeq \sin^2\theta_{12}\Delta m_{31}^2 + \cos^2\theta_{12}\Delta m_{32}^2 \\
- \sin2\theta_{12}\sin\theta_{13}\cot\theta_{23}\cos\delta\Delta m_{21}^2,
\end{aligned}
\tag{7}
$$

where terms at the order of $\mathcal{O}(\sin^2\theta_{13}\Delta m_{21}^2)$ have been neglected for simplicity. We can also calculate the differences of the effective quantities between different flavors as

$$
\begin{aligned}
|\Delta m_{ee}^2| - |\Delta m_{\mu\mu}^2| \\
= \pm\Delta m_{21}^2(\cos2\theta_{12} - \sin2\theta_{12}\sin\theta_{13}\tan\theta_{23}\cos\delta),
\end{aligned}
\tag{8}
$$

$$
|\Delta m_{\mu\mu}^2| - |\Delta m_{\tau\tau}^2| = \pm2\Delta m_{21}^2\sin2\theta_{12}\sin\theta_{13}\csc2\theta_{23}\cos\delta,
\tag{9}
$$

where the positive and negative signs correspond to normal and inverted mass hierarchies, respectively.

On the other hand, at the first oscillation maximum of the solar mass-squared difference, such as the reactor neutrino experiment at the medium baseline, we have the approximation of $\sin\Delta_{21} \sim 1$ and $\cos\Delta_{21} \sim 0$. Therefore, we can separate the fast and slow oscillation terms, if η_α fulfills the equation as

$$
\begin{aligned}
|U_{\alpha1}|^2 \cos[\eta_\alpha\Delta_{21}]\cos[2\Delta_{32} + \eta_\alpha\Delta_{21}] \\
+ |U_{\alpha2}|^2 \sin[\eta_\alpha\Delta_{21}]\sin[2\Delta_{32} + \eta_\alpha\Delta_{21}] = 0.
\end{aligned}
\tag{10}
$$

One should note that η_α depends on both the neutrino MH and the neutrino energy. The MH sensitivity is encoded in the energy dependence of $\Delta m_{\alpha\alpha}^2$. Moreover, because of the different definitions of $\Delta m_{\alpha\alpha}^2$ in these two oscillation scenarios, the MH sensitivity of the reactor neutrino experiment at the medium baseline can be improved by including the extra measurements of Δm_{ee}^2 in Eq. (5) and $\Delta m_{\mu\mu}^2$ in Eq. (6).
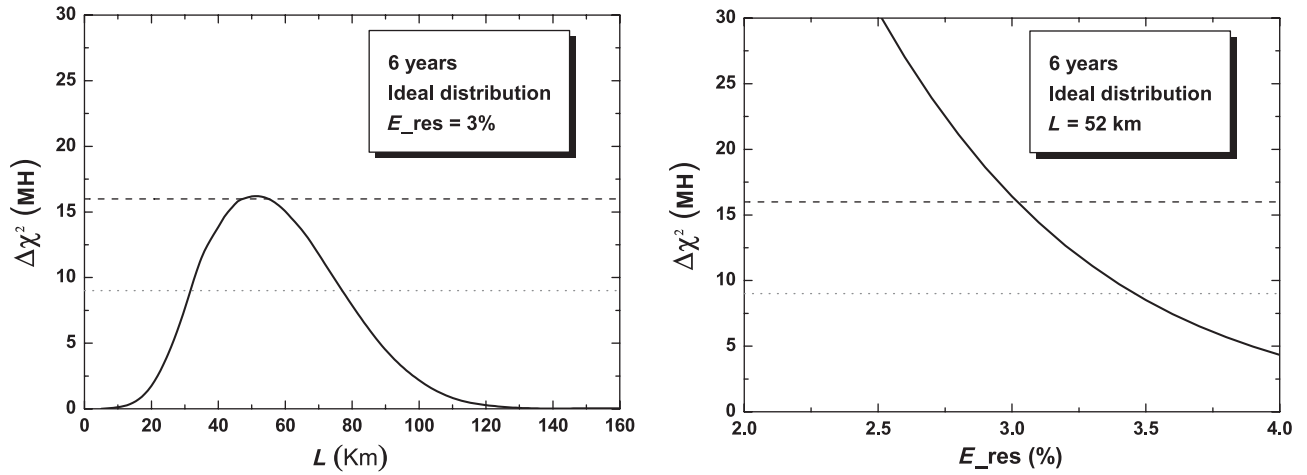
FIG. 1.   The MH discrimination ability for the proposed reactor neutrino experiment as functions of the baseline (left panel) and the detector energy resolution (right panel) with the method of the least-squares function in Eq. (11).

For a reactor neutrino experiment at the medium baseline, corrections to the mass-squared differences from the terrestrial matter effect are around 1% and the induced uncertainties are negligibly small (less than 0.1%). On the other hand, in the muon-neutrino disappearance channel of long-baseline accelerator neutrino experiments, the matter corrections are suppressed by the smallness of θ_{13} and only at the level of 0.2% for the baselines of several hundreds kilometers (e.g., 295 km for T2K [31] and 735 km for NOνA [32]). Moreover, the different signs in the matter potentials of neutrino and antineutrino oscillations are also favorable to increase the discrepancy of different mass-squared differences.

III. STATISTICAL ANALYSIS

The 20 kton liquid scintillator detector of the Daya Bay II experiment [19–21] will be located at equal baselines of 52 km away from two reactor complexes (36 GW in total). In this study we use a nominal running time of six years, 300 effective days per year, and a detector energy resolution $3\%/\sqrt{E \text{ (MeV)}}$ as a benchmark. A normal MH is assumed to be the true one (otherwise mentioned explicitly) while the conclusion will not be changed for the other assumption. The relevant oscillation parameters are taken from the latest global analysis [28] as $\Delta m_{21}^2 = 7.54 \times 10^{-5}$ eV^{-2}, $(\Delta m_{31}^2 + \Delta m_{32}^2)/2 = 2.43 \times 10^{-5}$ eV^{-2}, $\sin^2 \theta_{13} = 0.024$, and $\sin^2 \theta_{12} = 0.307$. The CP-violating phase will be specified when needed. Finally, the reactor antineutrino flux model from Vogel *et al.* [33] is adopted in our simulation.[1] Because two of the three mass-squared differences (Δm_{21}^2, Δm_{31}^2, and Δm_{32}^2) are independent, we choose

Δm_{21}^2 and Δm_{ee}^2 defined in Eq. (5) as the free parameters in this work.

To obtain the sensitivity of the proposed experiment, we employ the least-squares method and construct a standard χ^2 function as follows:

$$\chi^2_{\text{REA}} = \sum_{i=1}^{N_{\text{bin}}} \frac{[M_i - T_i(1 + \sum_k \alpha_{ik}\epsilon_k)]^2}{M_i} + \sum_k \frac{\epsilon_k^2}{\sigma_k^2}, \quad (11)$$

where M_i is the measured neutrino events in the ith energy bin, T_i is the predicted reactor antineutrino flux with oscillations, σ_k is the systematic uncertainty, ϵ_k is the corresponding pull parameter, and α_{ik} is the fraction of neutrino event contribution of the kth pull parameter to the ith energy bin. The considered systematic uncertainties include the correlated (absolute) reactor uncertainty (2%), the uncorrelated (relative) reactor uncertainty (0.8%), the flux spectrum uncertainty (1%), and the detector-related uncertainty (1%). We use 200 equal-size bins for the incoming neutrino energy between 1.8 and 8.0 MeV.

We can fit both the normal MH and inverted MH with the least-squares method and take the difference of the minima as a measurement of the MH sensitivity. The discriminator of the neutrino MH can be defined as

$$\Delta \chi^2_{\text{MH}} = |\chi^2_{\text{min}}(\text{N}) - \chi^2_{\text{min}}(\text{I})|, \quad (12)$$

where the minimization process is implemented for all the relevant oscillation parameters. Note that two local minima for each MH [$\chi^2_{\text{min}}(\text{N})$ and $\chi^2_{\text{min}}(\text{I})$] can be located at different positions of $|\Delta m_{ee}^2|$. This particular discriminator is used to obtain the optimal baseline and to explore the impact of the energy resolution, which are shown in the left and right panels of Fig. 1. Ideally a sensitivity of $\Delta \chi^2_{\text{MH}} \simeq 16$ can be obtained at the baseline around 50 km and with a detector energy resolution of 3%.

The baselines to two reactor complexes should be equal. The impact of unequal baselines is shown in the left panel of Fig. 2, by keeping the baseline of one reactor unchanged

---

[1]We have tried both the calculated [33] and the new evaluations [34,35] of the reactor antineutrino fluxes. The discrepancy only influences the measurement of θ_{12}. Both evaluations give consistent results on the MH determination.
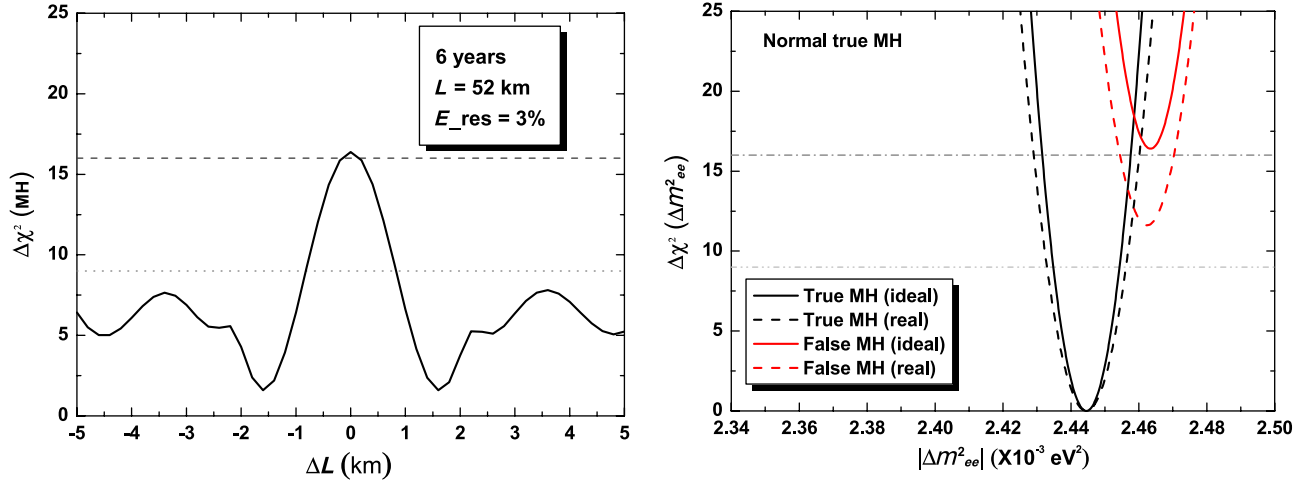
FIG. 2 (color online). The variation (left panel) of the MH sensitivity as a function of the baseline difference of two reactors and the comparison (right panel) of the MH sensitivity for the ideal and actual distributions of the reactor cores.

and varying that of another. A rapid oscillatory behavior is observed and demonstrates the importance of baseline differences for the reactor cores. To evaluate the impact from the spacial distribution of individual cores, we take the actual power and baseline distribution of each core of the Yangjiang (YJ) and Taishan (TS) nuclear power plant, shown in Table I. The remote reactors in the Daya Bay and the possible Huizhou (HZ) power plant are also included. The reduction of sensitivity due to the actual distribution of reactor cores is shown in the right panel of Fig. 2, which gives a degradation of $\Delta\chi^2_{\mathrm{MH}} \simeq 5$. In all the following studies, the actual spacial distribution of reactor cores for the Daya Bay II experiment is taken into account.

IV. ENERGY NONLINEARITY EFFECT

The detector energy response is also crucial for Daya Bay II since a precise energy spectrum of reactor neutrinos is required. Assuming the energy nonlinearity correction is imperfect, we study its impact to the sensitivity by including in our simulation a residual nonlinearity between the measured and expected neutrino spectra. Assume the detector energy nonlinearity has the form as

$$\frac{E_{\mathrm{rec}}}{E_{\mathrm{true}}} = \frac{1 + p_0}{1 + p_1 \exp{(-p_2 E_{\mathrm{true}})}}, \quad (13)$$

TABLE I. Summary of the power and baseline distribution for the Yangjiang and Taishan reactor complexes, as well as the remote reactors of Daya Bay and Huizhou.

Cores	YJ-C1	YJ-C2	YJ-C3	YJ-C4	YJ-C5	YJ-C6
Power (GW)	2.9	2.9	2.9	2.9	2.9	2.9
Baseline (km)	52.75	52.84	52.42	52.51	52.12	52.21
Cores	TS-C1	TS-C2	TS-C3	TS-C4	DYB	HZ
Power (GW)	4.6	4.6	4.6	4.6	17.4	17.4
Baseline (km)	52.76	52.63	52.32	52.20	215	265

where E_{rec} and E_{true} are the reconstructed and true kinematic energy of the positron from the inverse beta decay, respectively. The parameter of p_0, p_1, and p_2 describe the shape and magnitude of the nonlinear functions. We assume that, after the nonlinearity correction, the residual nonlinearity in the measured energy spectrum also has the same function form. The conclusion will not be changed for other residual nonlinearity assumptions because we will use a quadratic function in the predicted spectrum, different from the measured spectrum. We fix $p_2 = 0.2/\mathrm{MeV}$ and vary p_0 and p_1 as

$$p_0 = \mathrm{sign} \times \mathrm{size}_0 \quad \mathrm{and} \quad p_1 = \mathrm{sign} \times \mathrm{size}_1, \quad (14)$$

where $\mathrm{sign} = \pm 1$ determines the slope, and size_0 and size_1 can be a few percent to indicate the magnitudes of the residual nonlinearity. Two typical examples with $\mathrm{sign} = \pm 1$ are shown in Fig. 3.

By including the residual nonlinearity in M_i of Eq. (11), we obtain in Fig. 4 updates on the distributions of the $\Delta\chi^2$ function for both true and false neutrino MH, where normal (inverted) MH is assumed to be the true one in upper (lower) panels. Different classes of the nonlinear functions may induce different effects on the MH determination. Comparing to that without nonlinearity effects, as shown in the right panel of Fig. 2, the nonlinearity with positive sign (sign = +1) will increase the discrepancy between two neutrino MH scenarios for the normal true MH, but decrease the discrepancy for the inverted true MH. The nonlinear functions with negative sign (sign = −1) have opposite effect. Only when the size of nonlinearity is as small as 0.5% can this effect be ignored.

For the reactor antineutrino experiment at medium baseline (~ 50 km), we can observe multiple peaks of the Δm^2_{ee} induced oscillation. Each peak position carries the information of Δm^2_{ee}. This redundancy can be used to evaluate the energy scale at different energies. Therefore, we can measure to some extent the energy nonlinearity by the
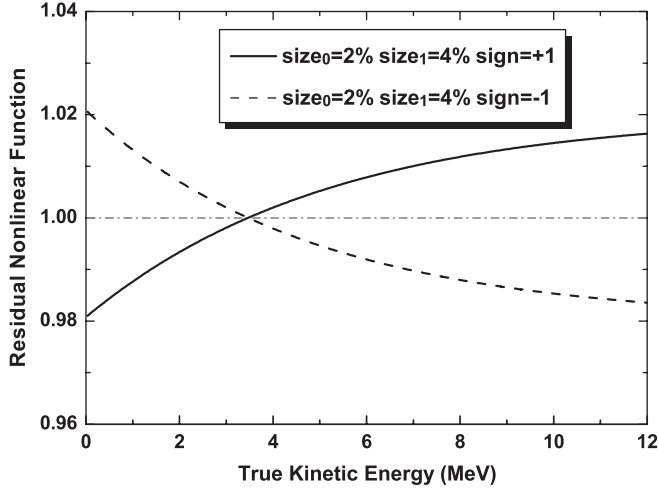
FIG. 3.   Two classes of typical examples for the residual nonlinear functions in our simulation.

spectrum itself. We call this effect the self-calibration of the spectrum. To illustrate, we consider a test quadratic nonlinear function in the fitting process,

$$\frac{E_{\text{rec}}}{E_{\text{true}}} \simeq 1 + q_0 + q_1 E_{\text{true}} + q_2 E_{\text{true}}^2, \qquad (15)$$

where the central values of three parameters are arbitrary, but the uncertainties are assumed to be the same size as the function in Eq. (13). We can define the new least-square function by using the test nonlinearity function in T_i and including the corresponding pull terms $\chi_{\text{NL}}^2 = \sum_{i=0}^{2} q_i^2/(\delta q_i)^2$, and we can derive the MH sensitivity by taking into account the nonlinearity and self-calibration effects. Considering different signs and sizes of nonlinearity defined in Eq. (13), we illustrate the $\Delta \chi^2$ function with the self-calibration in fitting in Fig. 5, where the normal (inverted) MH is assumed to be the true one in the upper (lower) panels. First we can observe that the degeneracy
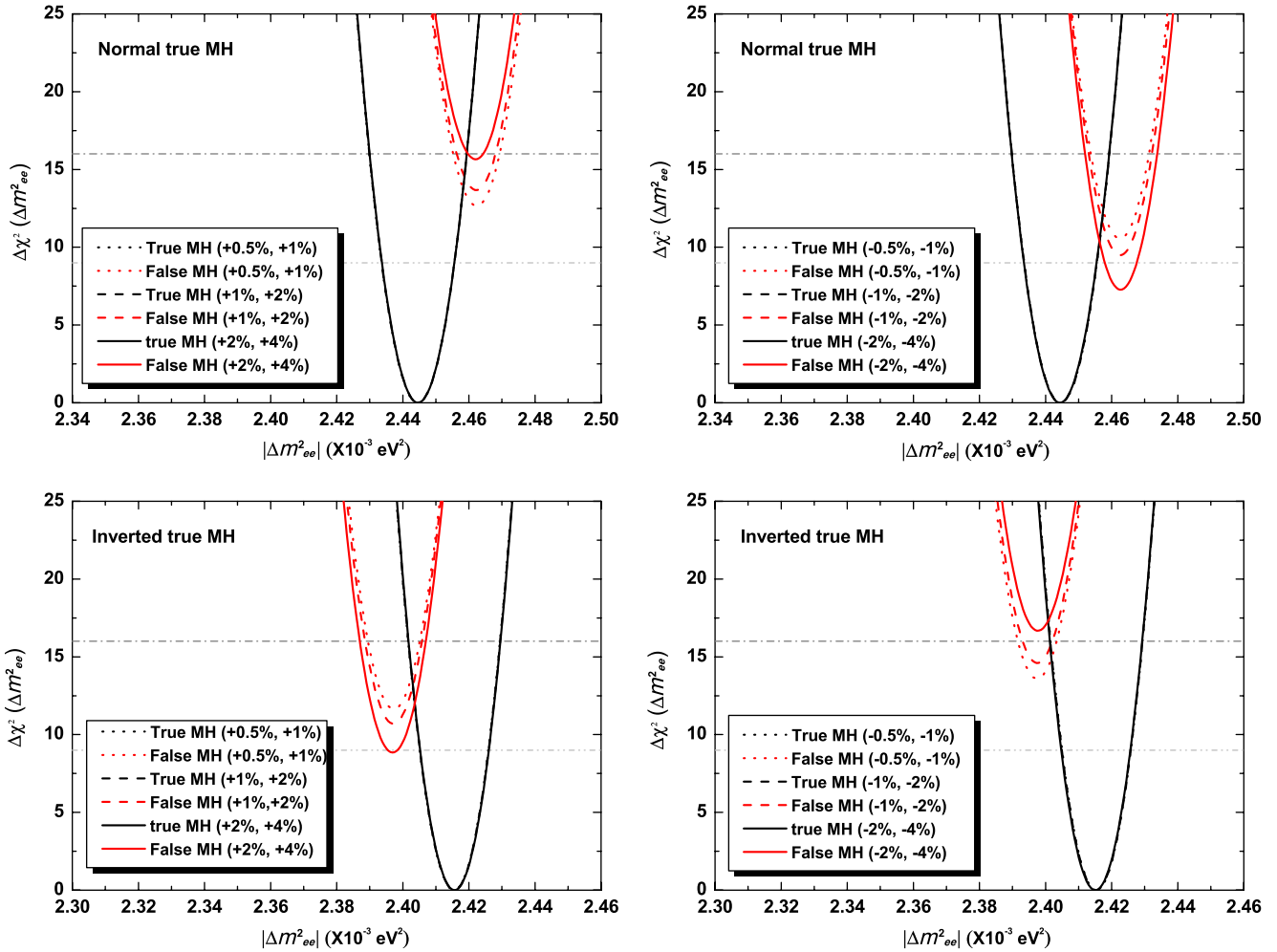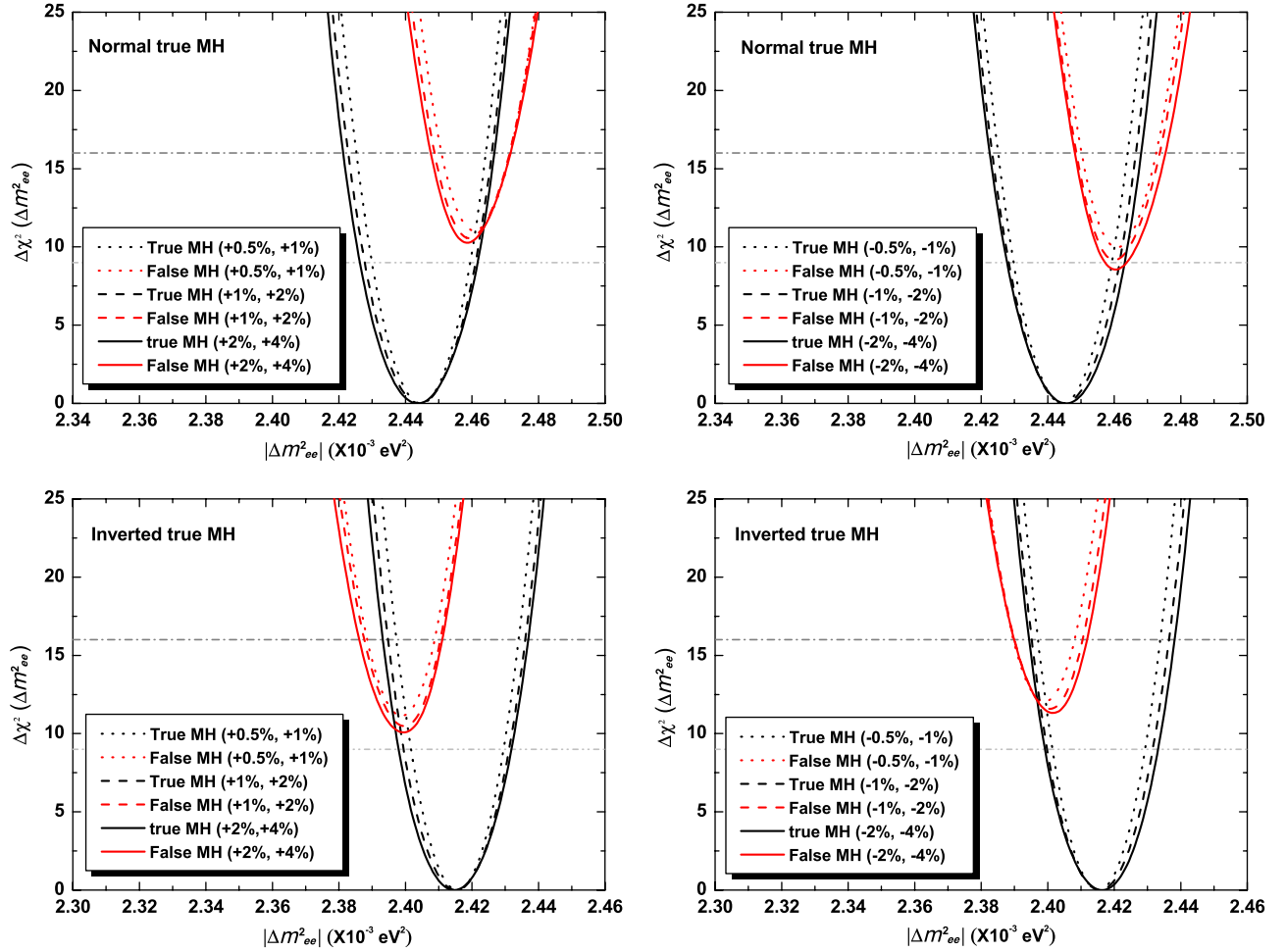

FIG. 4 (color online).   Effects of two classes of energy nonlinearity models in the determination of the neutrino MH without the self-calibration in fitting. The normal (inverted) MH is assumed to be the true one in the upper (lower) panels. The sign and size of the nonlinear parameters in the form of (p_0, p_1) are indicated in the legend.

FIG. 5 (color online). Effects of two classes of energy nonlinearity models in the determination of the neutrino MH with the self-calibration in fitting. The normal (inverted) MH is assumed to be the true one in the upper (lower) panels. The sign and size of the nonlinear parameters in the form of (p_0, p_1) are indicated in the legend.

ambiguity induced by the nonlinearity effect can be removed by fitting the parameters of the test nonlinearity function, and that both classes of nonlinear functions give the consistent sensitivity of MH determination (see the left and right panels of Figs. 4 and 5). Tiny differences can be noticed for different sizes of the nonlinearity because the test quadratic function cannot describe the true residual nonlinearity accurately. Second, the width of the $\Delta\chi^2$ functions in Fig. 5 is broadened compared to Fig. 4. This is because additional uncertainties from the nonlinearity parameters are introduced, which can be translated to the uncertainty of the neutrino spectrum and finally to the accuracy of the oscillation parameters.

V. IMPROVEMENT WITH EXTERNAL MEASUREMENTS

Taking into account different definitions of $\Delta m^2_{\alpha\alpha}$ in different oscillation scenarios, precise measurements of Δm^2_{ee} and $\Delta m^2_{\mu\mu}$ in Eqs. (5) and (6) can provide the additional MH sensitivity in Daya Bay II.

To incorporate the contributions of $\Delta m^2_{\mu\mu}$ from long-baseline accelerator neutrino experiments and Δm^2_{ee} from short-baseline reactor neutrino experiments, we define the following pull χ^2 function:

$$\chi^2_{\text{pull}} = \frac{(|\Delta m^2_{\mu\mu}| - \overline{|\Delta m^2_{\mu\mu}|})^2}{\sigma^2(\Delta m^2_{\mu\mu})} + \frac{(|\Delta m^2_{ee}| - \overline{|\Delta m^2_{ee}|})^2}{\sigma^2(\Delta m^2_{ee})},$$

(16)

where $\overline{\Delta m^2_{\mu\mu}}$ $(\overline{\Delta m^2_{ee}})$ and $\sigma(\Delta m^2_{\mu\mu})$ $[\sigma(\Delta m^2_{ee})]$ are the central value and 1σ uncertainty of the measurement, respectively. The combined χ^2 function is defined as

$$\chi^2_{\text{ALL}} = \chi^2_{\text{REA}} + \chi^2_{\text{pull}}.$$

(17)

As mentioned in the previous section, we choose Δm^2_{21} and Δm^2_{ee} defined in Eq. (5) as the free parameters. The values of $\Delta m^2_{\mu\mu}$ can be calculated by the relations in Eqs. (8) and (9) by assuming different choices of the MH.

In general we need to consider the uncertainties of other oscillation parameters, but the *CP*-violating phase δ is
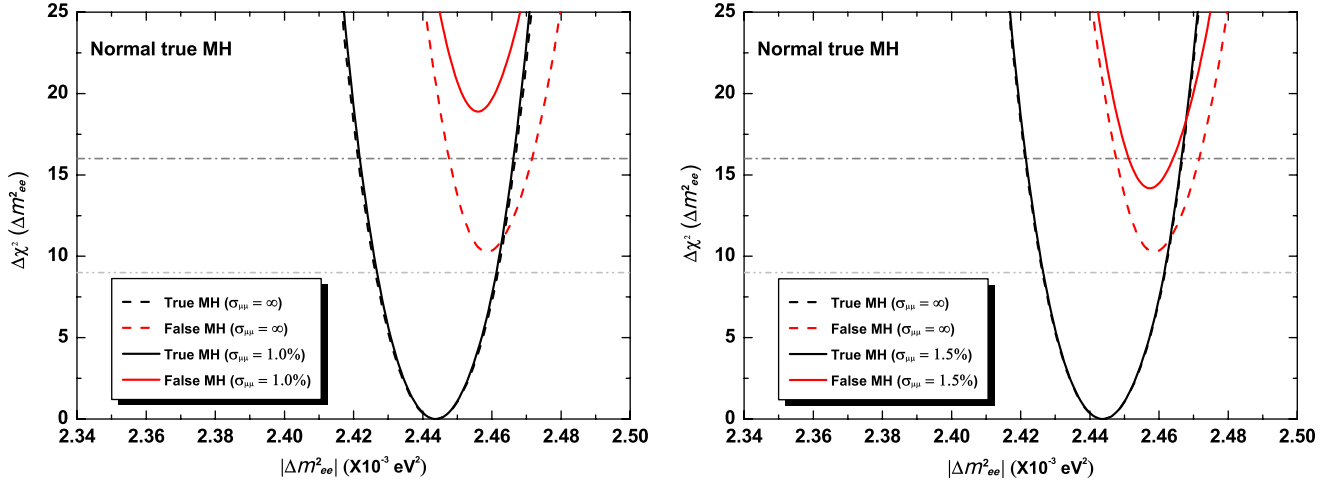
FIG. 6 (color online). The reactor-only (dashed) and combined (solid) distributions of the $\Delta\chi^2$ function in Eqs. (11) and (17), where a 1% (left panel) or 1.5% (right panel) relative error of $\Delta m^2_{\mu\mu}$ is assumed and the CP-violating phase (δ) is assigned to be $90°/270°$ ($\cos\delta = 0$) for illustration. The black and red lines are for the true (normal) and false (inverted) neutrino MH, respectively. The nonlinearity in Eq. (13) is assigned with sign $= +1$, size$_0 = 2\%$, and size$_1 = 4\%$.

almost unconstrained and we can absorb the uncertainties of other parameters in that of the phase δ and consider the whole range of CP-violating phase from $0°$ to $360°$. Until 2020, the most accurate measurement of Δm^2_{ee} may come from the Daya Bay experiment, where an accuracy of 4% [36] can be achieved after a three-year running of full operation. Numerical analysis demonstrates that the measurement of Δm^2_{ee} at this level is negligible in the χ^2 function in Eq. (16). Therefore, we focus on the effect of $\Delta m^2_{\mu\mu}$ in this work.

As shown in Eq. (8), because the relative size of Δm^2_{ee} and $\Delta m^2_{\mu\mu}$ is different for the normal and inverted neutrino MH, the extra pull function χ^2_{pull} in Eq. (16) can give a nonzero contribution to the discriminator $\Delta\chi^2_{\text{MH}}$ at the magnitude of

$$\chi^2_{\text{pull}}(\text{MH})$$
$$\sim \frac{[2 \times \Delta m^2_{21}(\cos 2\theta_{12} - \sin 2\theta_{12}\sin\theta_{13}\tan\theta_{23}\cos\delta)]^2}{\sigma^2(\Delta m^2_{\mu\mu})},$$
$$(18)$$

and accordingly improve the neutrino MH sensitivity for the reactor neutrino experiment at medium baseline.

To illustrate the effect of the external $\Delta m^2_{\mu\mu}$ measurement, we first fix the nonlinearity with sign $= +1$, size$_0 = 2\%$, and size$_1 = 4\%$, choose δ to be $90°/270°$ ($\cos\delta = 0$) and give the separated and combined distributions of the χ^2 functions in Eqs. (11) and (17) in Fig. 6, where a 1% (left panel) or 1.5% (right panel) relative error of $\Delta m^2_{\mu\mu}$ is assumed. The black and red lines are for the true (normal) and false (inverted) neutrino MH, respectively. The dashed and solid lines are for the reactor-only [in Eq. (11)] and combined distributions. We can get a value of $\Delta\chi^2_{\text{MH}} \simeq (10 \div 11)$ for the reactor-only analysis in the least-squares

method. As for the contribution from the external $\Delta m^2_{\mu\mu}$ measurement, it is almost negligible if we choose the true MH in the fitting program. However, if the fitting MH is different from the true one, the central value of Δm^2_{ee} in the χ^2_{pull} function will change by two units of the difference in Eq. (8), which accordingly results in a significant contribution to the combined χ^2 function. Finally we can achieve $\Delta\chi^2_{\text{MH}} \simeq 19$ and $\Delta\chi^2_{\text{MH}} \simeq 14$ for the 1% and 1.5% relative errors of the $\Delta m^2_{\mu\mu}$ measurement.

Next we can discuss the ambiguity of the unknown CP-violating phase δ and evolution of the MH sensitivity with respect to changes of the $\Delta m^2_{\mu\mu}$ error. The $\Delta\chi^2_{\text{MH}}$ dependence on different input errors is shown in Fig. 7,
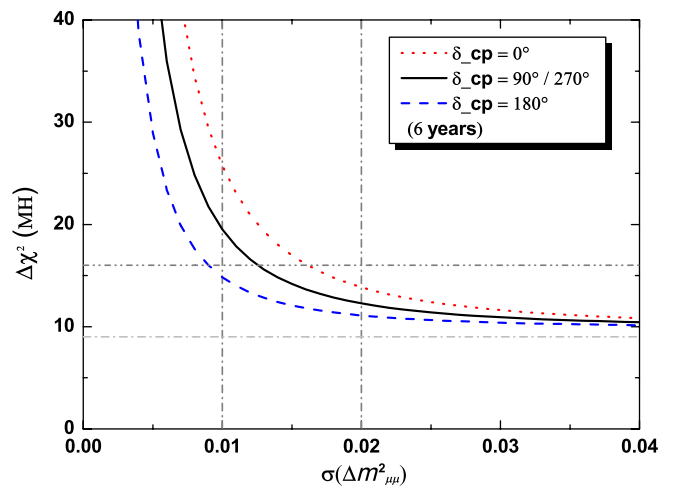

FIG. 7 (color online). The $\Delta\chi^2_{\text{MH}}$ dependence on different input errors of $\Delta m^2_{\mu\mu}$ is illustrated. The blue dashed, black solid, and red dotted lines stands for different CP values ($\delta = 0°$, $\delta = 90°/270°$, and $\delta = 180°$, respectively).

where the blue, black, and red lines stand for different values of the *CP*-violating phase ($\delta = 0°$, $\delta = 90°/270°$, and $\delta = 180°$, respectively). In Fig. 7, we can notice that the improvement is obvious for an external $\Delta m^2_{\mu\mu}$ measurement better than 2% and becomes significant if we can get to the 1% level. For the effect of the *CP*-violating phase, it is most favorable for the value close to 180°. The cases of maximal *CP* violation are in the middle region which are just the cases discussed in Fig. 6. The ambiguity of the *CP*-violating phase can induce an uncertainty of $\Delta\chi^2_{\mathrm{MH}} \simeq 2(4)$ at $\sigma(\Delta m^2_{\mu\mu})/|\Delta m^2_{\mu\mu}| \simeq 1.5\%(1\%)$. The effect of the external $\Delta m^2_{\mu\mu}$ measurement can also be viewed as a probe of the *CP*-violating phase. If the improvement is much better than the discussion in Fig. 6, a preference of δ close to 180° can be achieved. Otherwise, we may get a nearly vanishing *CP*-violating phase if the situation is totally opposite.

The current best measurement for $\Delta m^2_{\mu\mu}$ from the MINOS experiment [37] gives an error of 4%. Two new experiments T2K [31] and NOνA [32] are in operation or construction and each of them can reach 1.5% by 2020 after finishing their nominal running plans (five years of ν mode at 750 kW for T2K and three years of ν mode plus three years of $\bar{\nu}$ mode at 700 kW for NOνA). If these experiments could extend to another five-year running, it might be possible to obtain the precision of 1% which will be useful for the measurement of the precision reactor neutrino experiment.

VI. CONCLUSION

In this work, we have discussed the determination of the neutrino MH using the Daya Bay II reactor neutrino experiment at a medium baseline around 50 km away from reactors. Precision measurements of the reactor antineutrino spectrum can probe the interference effect of two fast oscillation modes (i.e., oscillations induced by Δm^2_{31} and Δm^2_{32}) and sensitive to the neutrino MH. The corresponding sensitivity depends strongly on the size of θ_{13}, the energy resolution, the baseline differences, and energy response functions. Moreover, the MH sensitivity can be improved by including a measurement of the effective mass-squared difference in the long-baseline muon-neutrino disappearance experiment due to flavor dependence of the effective mass-squared differences.

We have calculated the MH sensitivity, taking into account the real spatial distribution of reactor complexes, and demonstrated that the residual energy nonlinearity of the liquid scintillator detector has limited impacts on the sensitivity due to the self-calibration of small oscillation peaks. We numerically calculated the sensitivity by assuming two typical classes of energy nonlinearity functions (2%) and discussed the improvement with the external $\Delta m^2_{\mu\mu}$ measurement quantitatively. To conclude, the Daya Bay II experiment could determine the mass hierarchy unambiguously with a confidence level of $\Delta\chi^2_{\mathrm{MH}} \sim 14$ (3.7σ) or $\Delta\chi^2_{\mathrm{MH}} \sim 19$ (4.4σ) in six years, for the $\Delta m^2_{\mu\mu}$ uncertainty of 1.5% or 1%.

[1] F. P. An *et al.* (Daya Bay Collaboration), Phys. Rev. Lett. **108,** 171803 (2012).
[2] F. P. An *et al.* (Daya Bay Collaboration), Chinese Phys. C **37,** 011001 (2013).
[3] Y. Abe *et al.* (Double Chooz Collaboration), Phys. Rev. Lett. **108,** 131801 (2012).
[4] J. K. Ahn *et al.* (RENO Collaboration), Phys. Rev. Lett. **108,** 191802 (2012).
[5] K. Abe *et al.* (T2K Collaboration), Phys. Rev. Lett. **107,** 041801 (2011).
[6] P. Adamson *et al.* (MINOS Collaboration), Phys. Rev. Lett. **107,** 181802 (2011).
[7] K. Abe *et al.* (HyperK Collaboration), arXiv:1109.3262.
[8] T. Akiri *et al.* (LBNE Collaboration), arXiv:1110.6249.
[9] S. Bertolucci *et al.*, arXiv:1208.0512.
[10] A. Samanta, Phys. Lett. B **673,** 37 (2009); Phys. Rev. D **81,** 037302 (2010).
[11] D. J. Koskinen, Mod. Phys. Lett. A **26,** 2899 (2011).
[12] S. T. Petcov and M. Piai, Phys. Lett. B **533,** 94 (2002).
[13] S. Choubey, S. T. Petcov, and M. Piai, Phys. Rev. D **68,** 113006 (2003).
[14] J. Learned, S. Dye, S. Pakvasa, and R. Svoboda, Phys. Rev. D **78,** 071302 (2008).
[15] L. Zhan, Y. Wang, J. Cao, and L. Wen, Phys. Rev. D **78,** 111103 (2008).
[16] L. Zhan, Y. Wang, J. Cao, and L. Wen, Phys. Rev. D **79,** 073007 (2009).
[17] P. Ghoshal and S. T. Petcov, J. High Energy Phys. 03 (2011) 058.
[18] S. F. Ge, K. Hagiwara, N. Okamura, and Y. Takaesu, J. High Energy Phys. 05 (2013) 131.
[19] Y. F. Wang, in *ICFA Seminar, Neutel 2011, Venice, Italy, 2008* (NuFact, Williamsburg, VA, 2012).
[20] J. Cao, in NeuTel 2009, OCPA 7, Kaohsiung, Taiwan; NuTurn 2012, Gran Sasso, Italy; ICHEP 2012, Melbourne, Australia; NPB 2012, Shen Zhen, China; VCI 2013, Vienna, Austria.
[21] L. Zhan, in NOW 2012, Lecce, Italy; C. G. Yang, in Numass 2013, Milano, Italy; Z. M. Wang, in Nu Geoscience 2013, Takayama, Japan.
[22] E. Ciuffoli, J. Evslin, and X. Zhang, J. High Energy Phys. 12 (2012) 004.
[23] X. Qian, D. A. Dwyer, R. D. McKeown, P. Vogel, W. Wang, and C. Zhang, Phys. Rev. D **87,** 033005 (2013).
[24] H. Nunokawa, S. Parke, and R. Z. Funchal, Phys. Rev. D **72,** 013009 (2005).

[25] A. de Gouvea, J. Jenkins, and B. Kayser, Phys. Rev. D **71**, 113009 (2005).

[26] X. Guo *et al.* (Daya Bay Collaboration), arXiv:hep-ex/0701029.

[27] J. Beringer *et al.* (Particle Data Group), Phys. Rev. D **86**, 010001 (2012).

[28] G. L. Fogli, E. Lisi, A. Marrone, D. Montanino, A. Palazzo, and A. M. Rotunno, Phys. Rev. D **86**, 013012 (2012).

[29] D. V. Forero, M. Tortola, and J. W. F. Valle, Phys. Rev. D **86**, 073012 (2012).

[30] M. C. Gonzalez-Garcia, M. Maltoni, J. Salvado, and T. Schwetz, J. High Energy Phys. 12 (2012) 123.

[31] M. Aoki, Nucl. Phys. B, Proc. Suppl. **111**, 146 (2002).

[32] I. Ambats *et al.* (NOνA), arXiv:hep-ex/0503053.

[33] P. Vogel, G. K. Schenter, F. M. Mann, and R. E. Schenter, Phys. Rev. C **24**, 1543 (1981).

[34] T. A. Mueller *et al.*, Phys. Rev. C **83**, 054615 (2011).

[35] P. Huber, Phys. Rev. C **84**, 024617 (2011).

[36] J. Cao, in *XV International Workshop on Neutrino Telescopes, 2013* (unpublished).

[37] P. Adamson *et al.* (MINOS Collaboration), Phys. Rev. Lett. **106**, 181801 (2011).